Results:

The interaction of DBC2 with the Hsp90 Chaperone machine

DBC2 was previously identified as a Cdc37-interacting protein by MALDI-TOF MS peptide mass finger printing of proteins pulled down with anti-Flag antibodies from extracts prepared from K562 cells transfected with Flag-tagged Cdc37 (Thomas Prince, not shown). The interaction was confirmed by verifying that Hsp90 and Cdc37 were co-adsorbed with Flag-tagged DBC2 generated by coupled transcription/ translation (TnT) in rabbit reticulocyte lysate (RRL) (Thomas Prince, not shown).

To determine whether DBC2 interacted with Hsp90 independently or in concert with other components of the Hsp90 chaperone machine (Figure 1a), [^{35}S]-labeled DBC2 containing an N-terminal Flag-epitope tag was synthesized by TnT in RRL and immuno-adsorbed by the addition of M2 anti-Flag agarose. Reactions were carried out in the presence or absence of Hsp90 inhibitors geldanamycin (GA) and sodium molybdate with DMSO and water as the vehicle controls. Immunoadsorbed proteins were separated on a SDS-PAGE and Western blotted for the presence of co-adsorbing components of the Hsp90 chaperone machine (figure 1a,b). In the presence of no additions (N.A, water) or DMSO, Hsp90 and Hsc70 were observed to co-adsorb with DBC2. In the presence of GA, DBC2's interactions with Hsp90, Hsc70 and Hop were enhanced, which is consistent with GA's known ability to stabilize client protein interactions with "intermediate" components of the Hsp90 machine (figure 1b). Addition of molybdate enhanced DBC2's interaction with Hsp90, and reduced its interaction with Hsc70 to below control levels, which is consistent with molybdate's ability to stabilized "late"

Hsp90 complexes that lack Hsc70 and HOP. In addition, in the presence of molybdate a slight interaction of DBC2 with Cdc37 was observed.

Buffer containing high salt concentrations (e.g., 0.5 M NaCl) strips Hsc70 and Hsp90 of associated co-chaperones. When DBC2 immunadsorptions from TnT RRL containing no additions or DMSO were washed with buffer containing 0.5 M NaCl, a barely perceptible interaction of DBC2 with Hsc70 was detected upon Western blotting. In the presence of GA, high salt buffer stripped Hsp90 and HOP from DBC2, with Hsc70 binding remaining stably bound. Molybdate stabilized the binding of Hsp90 with DBC2, while Hsc70 and Cdc37 were stripped from the complex. These findings suggest that in the presence of GA, DBC2 is bound to Hsc70's substrate binding site, while in the presence of molybdate DBC2 has been released from Hsc70 and occupies Hsp90's client binding site.

A

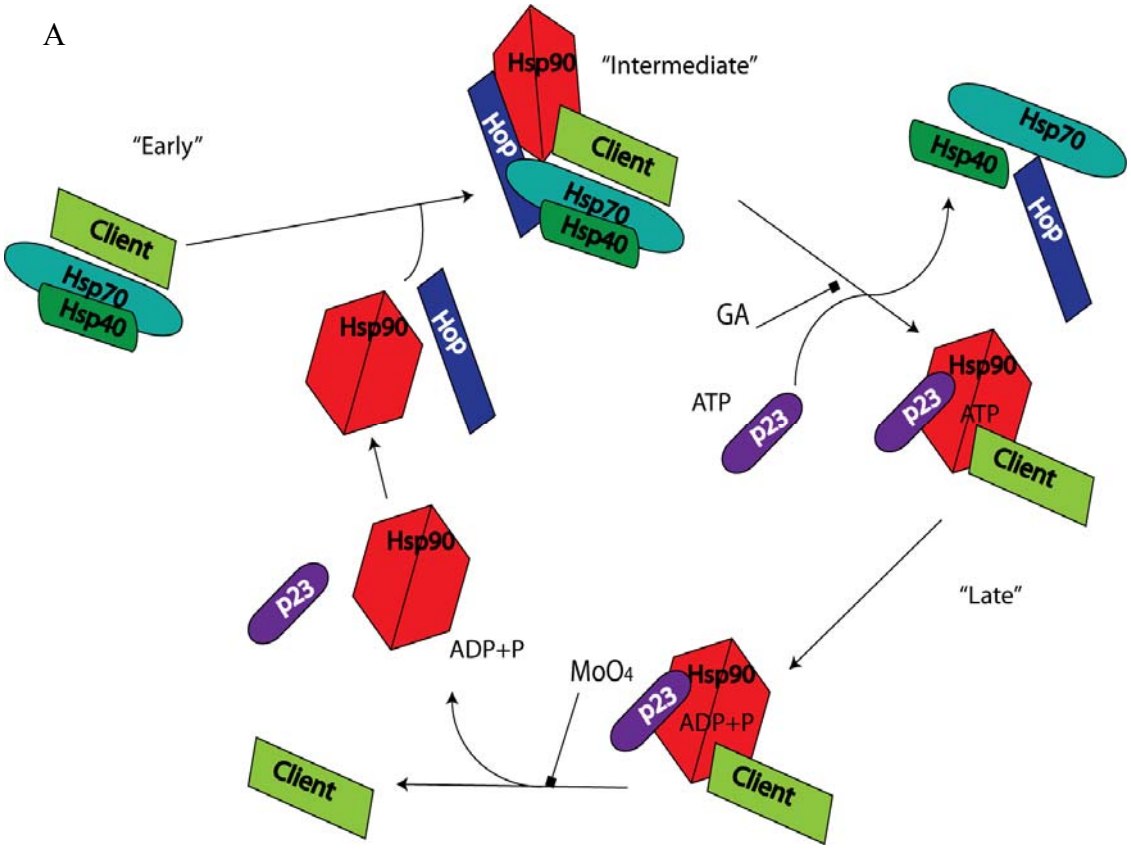
"Early"
"Intermediate"
"Late"
Client
Hsp70
Hsp40
Hsp90
Hop
GA
ATP
p23
ADP+P
MoO4

B

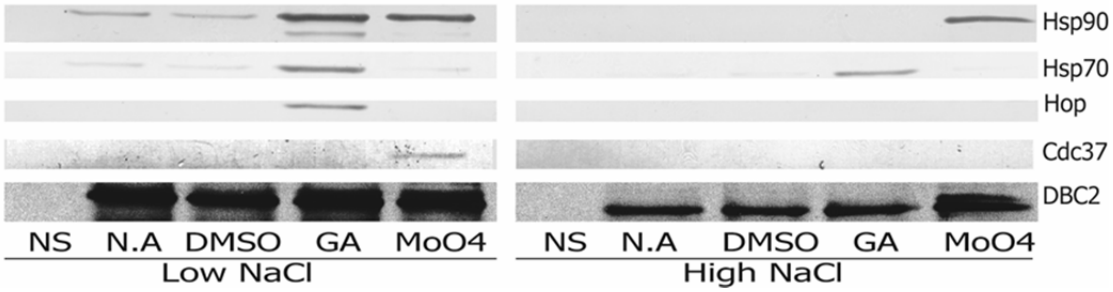
Hsp90
Hsp70
Hop
Cdc37
DBC2
NS
N.A
DMSO
GA
MoO4
Low NaCl
High NaCl

Figure 1. **Interaction of the Hsp90 chaperone machine with newly synthesized DBC2.** A.) Theoretical model of the Hsp90 Chaperone Cycle B.)^{35}S-labeled Flag-tagged DBC2 was synthesized in the presence or absence of geldanamycin or molybdate and immunoabsorbed from rabbit reticulocyte lysate with anti-Flag antibodies, as described in Experimental procedures. Immunoabsorbed samples were washed with buffer containing low (100 mM NaCl) or high salt (500 mM NaCl), as described in Experimental procedures. Samples were analyzed by SDS-PAGE, autoradiography (bottom panel) and Western blotting for co-absorption of endogenous Hsp90, Hsp70, Hop and Cdc37 (top to middle panel).

The interaction of DBC2 deletions construct with the Hsp90 chaperone machine

Previous work in the field has demonstrated that Hsp90's interaction with clients is usually localized to one, but sometimes two, domains of the client (Johnson et al., 2000). Therefore, deletion constructs of DBC2 were constructed to analyze the domains and/or motifs present in DBC2 that interacted with Hsp90 and components of its chaperone machine. [^{35}S]-Labeled Flag-tagged DBC2 and DBC2 deletion constructs were synthesized, immunoadsorbed with Anti-Flag agarose and analyzed for co-adsorbed components of the Hsp90 chaperone machinery as described above. Again, reactions were carried out in the presence or absence of Hsp90 inhibitors GA and sodium molybdate with DMSO and water as the vehicle controls. The deletions constructs are shown in Figure 2A with reference to the major DBC2 domains and sequence motifs. HOP and Hsc70, components of intermediate Hsp90 complexes interacted with the full-length DBC2, but their interactions were significantly reduced upon deletion of the N-terminal Rho domain. The interaction of the DBC2 deletion constructs with Hsp90 remains at a level nearly equivalent to that of Hsp90's interaction with full length DBC2 until the deletion of the first "split" BTB domain (Fig. 2B), with complete loss of Hsp90 binding being associated with the deletion of the second BTB domain. It should be noted that deletion of the linker region between the two BTB domains resulted in a significant reduction in Hsp90 binding (Fig. 2B, N501). Deletion of the Rho domain enhanced the binding of Cdc37 (the protein that was used to initially identify DBC2 as a putative Hsp90 client) to the N258, N297, N319 and the N351 constructs compared to full length DBC2, but this interaction was lost upon deletion of the linker that connects the bipartite BTB domain.

The results above indicated that the presence of the N-terminal Rho domain was necessary for the strong interaction of DBC2 with Hsp90 intermediate complex components Hsc70 and HOP. To determine whether the Rho domain retained the capacity to interact with Hsp90, Hsc70 and HOP, [^{35}S]labeled Flag-tagged DBC2 Rho domain (CΔ210) was synthesized, immunadsorbed to anti-Flag agarose in the presence or absence of Hsp90 inhibitors GA and sodium molybdate with DMSO and water as the vehicle controls, and analyzed for co-adsorbing proteins. The Western blot analysis showed the Hsp90, Hsc70 and HOP interacted with the isolated Rho domain (CΔ210) in a manner equivalent to their interactions with full length DBC2, indicating that it is the minimal domain required for binding of components of Hsp90 intermediate complex (fig. 2C). Thus, full-length DBC2 and its Rho domain showed hallmarks of Hsp90 clients, exhibiting characteristics changes in their interactions with components of the Hsp90 chaperone machine in response to the Hsp90 inhibitors GA and MoO_4. However, additional Hsp90 motifs must exist within the other domains, as interaction with Hsp90 was maintained by other DBC2 deletion constructs, albeit with significantly diminished interaction with Hsc70 and HOP and enhanced interactions with Cdc37.

A

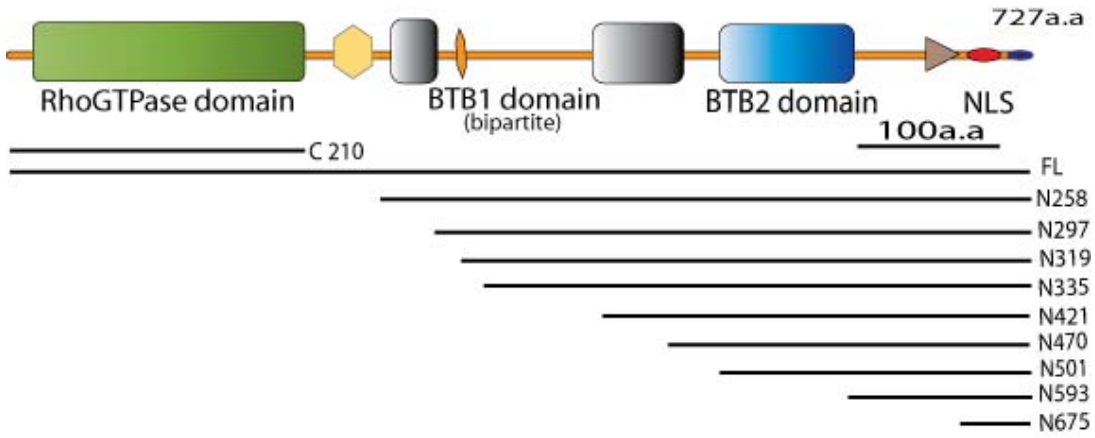
727a.a
RhoGTPase domain
BTB1 domain
(bipartite)
BTB2 domain
NLS
100a.a
C 210
FL
N258
N297
N319
N335
N421
N470
N501
N593
N675

B

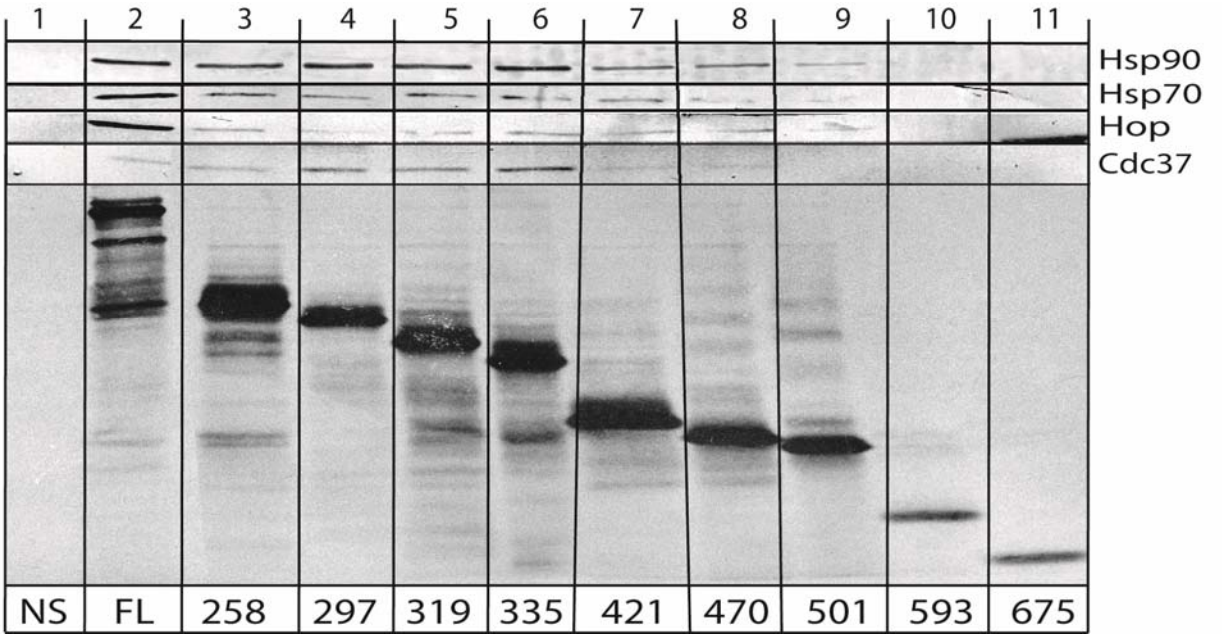
1
2
3
4
5
6
7
8
9
10
11
Hsp90
Hsp70
Hop
Cdc37
NS
FL
258
297
319
335
421
470
501
593
675

C

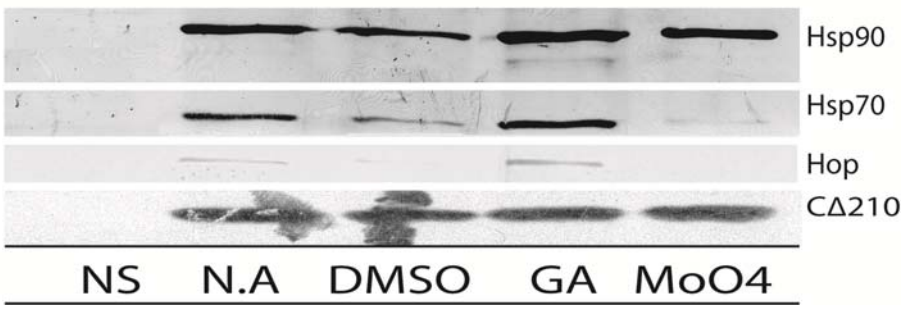
Hsp90
Hsp70
Hop
CΔ210
NS
N.A
DMSO
GA
MoO4

Figure 2. **Summary of the Flag-tagged DBC2 deletion constructs used for analysis of the Hsp90 chaperone machine interactions**. (A) Placement of C-terminal (Ct) and N-terminal (Nt) constructs of DBC2 relative to conserved structural motifs and domains, were positioned according to SMART, PFRAM and sequence alignments. The numbers flanking each line indicates the last residue for Ct deletion and the first for Nt deletions. Major domains are labeled with the Pro rich region containing the PEST motif in yellow, His rich region in orange, NLS in red, and the Ser rich element in dark blue with the putative RING domain as the brown triangle. (B) ^{35}S-labeled Flag-tagged full-length (FL) DBC2 and Flag-tagged DBC2 N-terminal deletion constructs, or (C) ^{35}S-labeled Flag-tagged Isolated DBC2 Rho domain (CΔ210) was synthesized in the presence or absence of geldanamycin or molybdate and immunoabsorbed from rabbit reticulocyte lysate with anti-Flag antibodies, as described in Experimental procedures. Immunoabsorption were washed with buffer containing low salt (100 mM NaCl), as described in Experimental procedures. Samples were analyzed by SDS-PAGE, autoradiography (bottom panels, B &C) and Western blotting for co-absorption of endogenous Hsp90, Hsp70, Hop and Cdc37 (Top & middle panel) or (C) endogenous Hsp90 and Hsp70 (top panel).

The GTP binding capacity of DBC2

While carring out the domain dissection of DBC2 we aligned DBC2 with other Rho family small G-proteins and the analysis indicated that previous work carried out on DBC2's capacity to bind GTP was done with a domain construct that lacked the G5 motif (Table 1; figure 3a), as its guanine nucleotide binding domain was truncated to a Ras domain (Paduch et al., 2001). The structural significance of truncating a Rho to a Ras domain (Figure 3a) lead us to re-examine the reported absence of GTP binding capacity of the DBC2 Rho domain (Chang et al., 2006). The DBC2 Rho domain is shown to have retained the necessary sequence features to bind GTP as shown by the alignment in Table 1. The small deviations from the consensus residues are shown in other atypical GTPases that have retain the ability to bind GTP even with mutations that rendered the ancestral Ras nonfunctional (Paduch et al. 2001). [^{35}S]-Labeled DBC2 was generated by TnT in RRL, incubated with GTP- or GMP-agarose, which was subsequently washed and assayed for bound DBC2 by SDS-PAGE and autoradiography. DBC2 was observed to specifically interact with GTP, but not GMP-agarose (Fig. 3b). Subsequently, we examined whether the GTP binding capacity was localized to its Rho domain. DBC2, its Rho domain (CΔ210) and DBC2ΔRho were generated by TnT and assayed for their capacity to bind GTP-agarose. DBC2 and its Rho domain specifically bound to the GTP-linked agarose at similar levels, while little binding of DBC2ΔRho (NΔ258) to GTP-agarose was observed (Fig. 3c). Thus, the GTP binding capacity of DBC2 is localized to its Rho domain. Also, a mutant of the full-length DBC2 with a R99G substitution, which is in the switch II region, was observed to have increased GTP binding compared to the

wild-type DBC2 and its isolated Rho domain (Fig. 3c), suggesting that the mutation may have increased the access of GTP to the binding cleft.

Protein	Sequence	G1 (p-loop)	G2 (switch I)	G3 (Switch II)	G4	G5
DBC2	O94844	GDNAVGKT	PTV	DTFGHH	CQLD	TSV
RhoBTB1	Q9BYz6	GDNAVGKT	PTV	DTFGHH	CQLD	TSV
Rac1	P63000	GDGAVGKT	PTV	DTAGQE	TKLD	CSA
Cdc42	P60953	GDGAVGKT	PTV	DTAGQE	TQLD	CSA
RhoA	P61585	GDGACGKT	PTV	DTAGQE	NKKD	CSA
Rap1A	P62834	GSGGVGKS	PTI	DTAGTE	NKCD	SSA
H-Ras	P01112	GAGGVGKS	PTI	DTAGQE	NKCD	TSA
Ran	P62826	GDGGTGKT	ATL	DTAGQE	NKVD	FVA
Rnd1	Q92730	GDVQCGKT	PTV	DTSGSP	CKTD	GSA
Rnd3	P61587	GDSQCGKT	PTV	DTSGSP	CKSD	CSA
RhoU	Q7L0Q8	GDGAVGKT	PTA	DTAGQD	TQSD	CSA
RhoH	Q15669	GDSAVGKT	PTV	DTAGND	TQTD	CSA
Consensus		(GXXXXGKT)	(XTX)	(DXXG)	(N/T)(K/Q)XD	(T/G/C)(C/S)A

Table 1. Consensus motifs that define a small GTPase domain, which confer structural and enzymatic support. Yellow indicates identical residues.

A

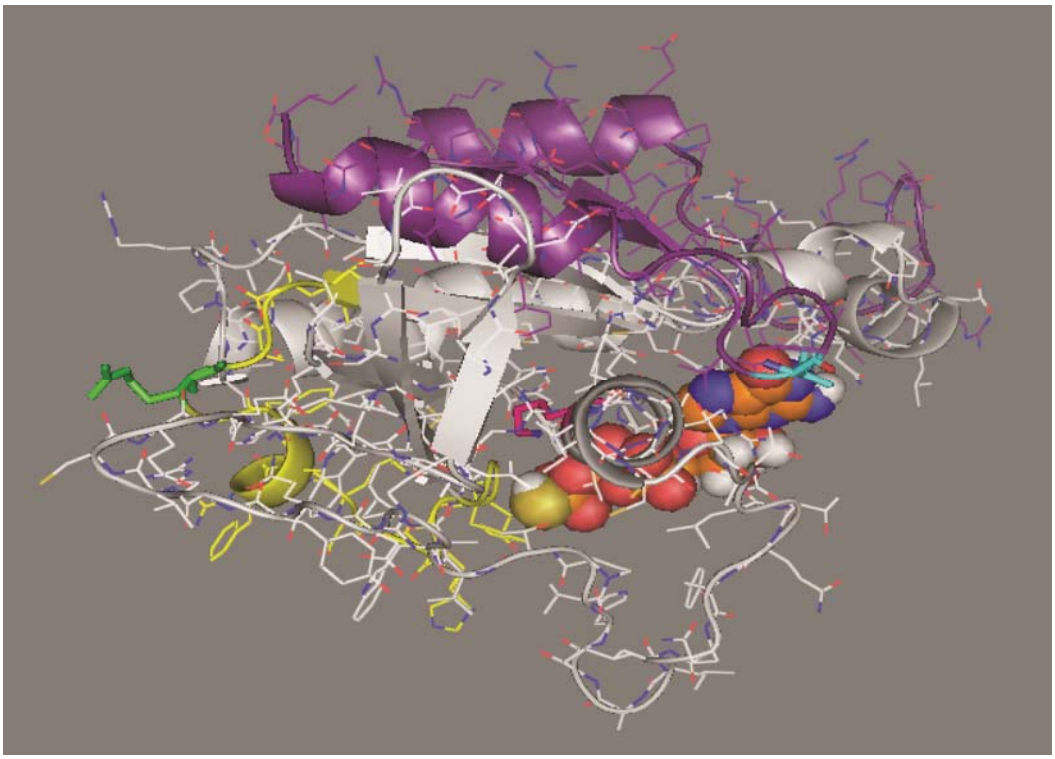

B

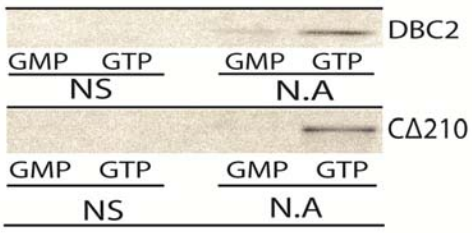
DBC2
GMP GTP
NS
GMP GTP
N.A
CΔ210
GMP GTP
NS
GMP GTP
N.A

C

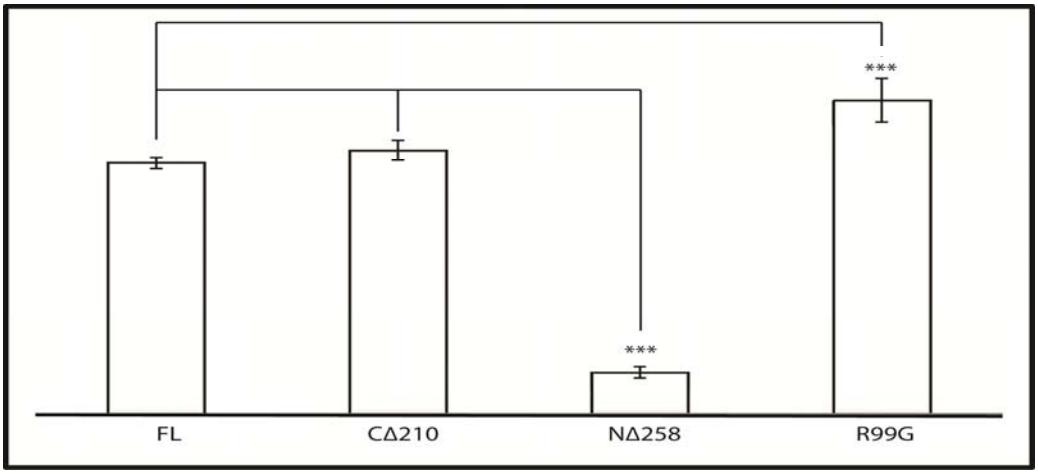
***
***
FL
CΔ210
NΔ258
R99G

Figure 3. **GTP binding elements and the Ras-like truncation of the DBC2 Rho domain.** (A) Homology model by Swiss-model of the DBC2 Rho domain. In purple are the 46 residues which are deleted when truncated to a Ras domain including the loss of the G5 loop (Chang et al., 2006). The switch II is colored yellow with the R99 residue in green. GTS is shown as spheres with V191 in light blue and K27 in pink. The image was rendered by PyMol , Delano scientific. (B)**[**^{35}S]-labeled Flag-tagged DBC2 and CΔ210 were synthesized and pulled down from rabbit reticulocyte lysate with GMP or GTP-linked agarose, as described in Experimental procedures. Pull down samples were washed with low salt wash buffer, as described in Experimental procedures. Samples were analyzed by SDS-PAGE, autoradiography (C) [^{35}S]-Labeled WT DBC2, DBC2 Rho domain (C210) and the DBC2ΔRho (N258) were generated by TnT followed incubation with GTP-agarose. The GTP-agarose pellets were then washed as described in Experimental procedures. The amount of bound [^{35}S]-DBC2 constructs were quantitated by scintillation counting and normalized for the number of Met in each construct (to WT) and for [^{35}S]-Met non-specifically bound to the GTP-agarose. The data represent three independent bio-replicates including three technical replicates. The (***) denotes a significant difference based on a 95% confidence interval, $P<0.05$.

The effect of Hsp90 inhibitors on GTP binding of the wild-type and the isolated Rho domain of DBC2

Since Hsp90 chaperone machine is required for client proteins to fold into an active/ functional conformation, the effect of Hsp90 inhibition on the GTP binding capacity of DBC2 was examined. The Hsp90 specific inhibitor geldanamycin significantly reduced the capacity of DBC2 to bind to GTP-agarose, while molybdate enhanced its ability to bind GTP-agarose relative to the vehicle controls (Fig. 4b). Washing the GTP-agarose resin with buffers containing 0.5 M NaCl (high salt) reduced the binding of DBC2 to the resin, but the observed trend of the effect of Hsp90 inhibition was still observed (Fig. 4b). Thus, Hsp90 appears to modulate DBC2's GTP binding capacity.

The results above indicate that both the DBC2 and its Rho domain bind GTP. Since DBC2's interaction with the Hsp90 chaperone machine also localized to the Rho domain, the effect of Hsp90 inhibitors on the GTP binding capacity of the Rho domain was examined next. While DBC2's Rho domain showed a small amount of reduction in its GTP binding capacity when Hsp90 was inhibited by the addition of geldanamycin (figure 4c), the reduction in binding was far less pronounced than that of full-length DBC2 (figure 4b.) Furthermore, molybdate cause no significant increase in the GTP binding capacity of DBC2's Rho domain (figure 4d). Thus, Hsp90 appears to modulate the GTP binding capacity of DBC2 primarily in the context of the full length protein.

A

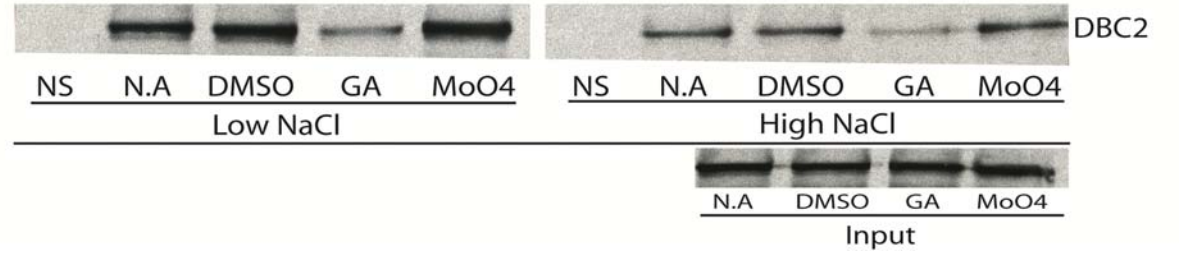
DBC2
NS N.A DMSO GA MoO4
NS N.A DMSO GA MoO4
Low NaCl
High NaCl
N.A DMSO GA MoO4
Input

B

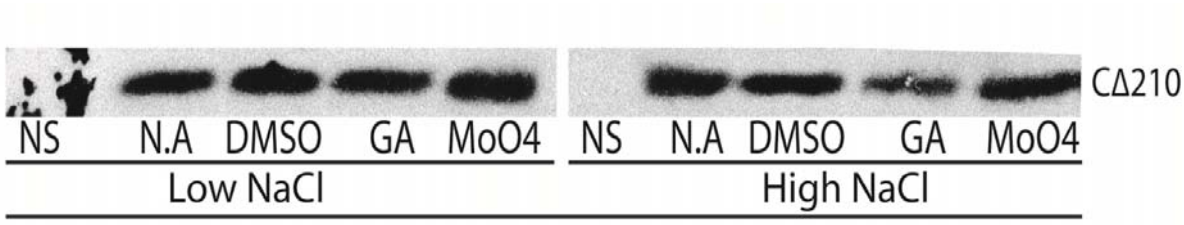
CΔ210
NS N.A DMSO GA MoO4
NS N.A DMSO GA MoO4
Low NaCl
High NaCl

C

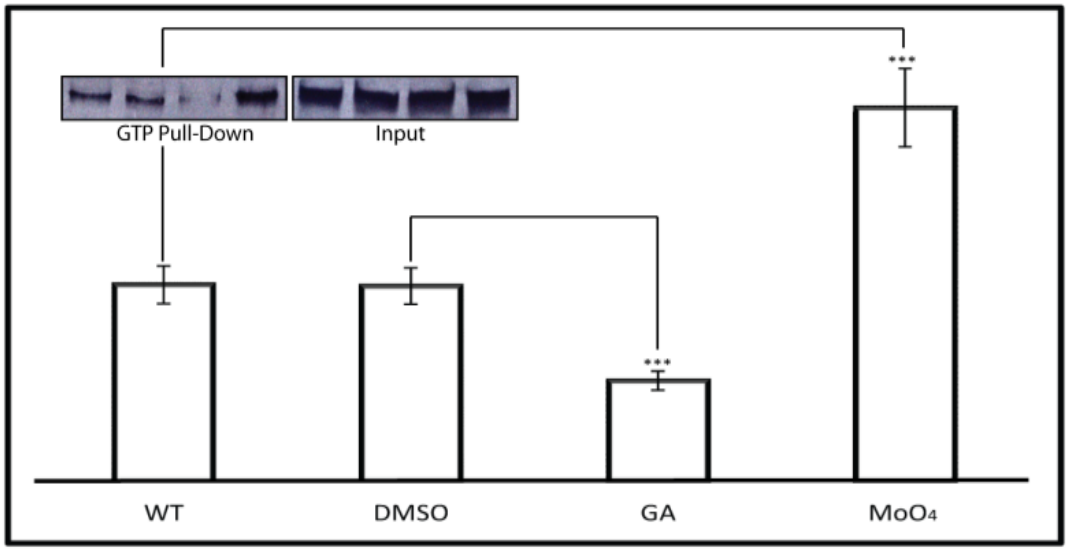
GTP Pull-Down
Input
***
***
WT
DMSO
GA
MoO4

Figure 4: **The Hsp90 effects on GTP binding to DBC2**. (A) [^{35}S]-labeled Flag-tagged DBC2 was synthesized in the presence or absence of geldanamycin or molybdate and pulled down from rabbit reticulocyte lysate with GTP-linked agarose, as described in Experimental procedures. Pull down (PD) samples were washed with buffer containing low(100 mM) or high (500 mM) NaCl wash, as described in Experimental procedures. Naïve reticulocyte lysate containing no template DNA was used as the control for nonspecific binding. Samples were analyzed by SDS-PAGE, autoradiography (bottom panel) and Western blotting for co-absorption of endogenous Hsp90 (top panel). Input: control for amounts of protein that was present in samples used for pulled down analyzed by SDS-PAGE and autoradiography. (B.) [^{35}S]-labeled Flag-tagged DBC2 carried out as in (A.) (C) in the presence or absence of geldanamycin or molybdate and pulled down from rabbit reticulocyte lysate with GTP-linked agarose, as described in Experimental procedures. The GTP-agarose pellets were then washed as described in Experimental procedures. The amount of bound [^{35}S]-DBC2 constructs were quantitated by scintillation counting and normalized and for [^{35}S]-Met non-specifically bound to the GTP-agarose. The data represent three independent bio-replicates including three technical replicates. The (***) denotes a significant difference based on a 95% confidence interval, $P<0.05$.

The effects of point mutations in the Rho domain of DBC2

The DBC2 mutant R99G, which increased the protein's capacity to bind GTP, was created serendipitously through PCR of DBC2. Molecular modeling suggest that a V191I mutation in the G5 loop of the GTP binding pocket should reduce or block the ability of the mutant to bind GTP. The ability of the R99G and V191I to specifically bind GTP-agarose was tested as described above using GMP agarose as the control. Both DBC2/R99G and DBC2/V191I were found to bind specifically to GTP-agarose, while a low level of non-specific binding to GMP-agarose was observed (Fig 5a). Again a significant increase in the binding of the R99G mutant to GTP-agarose was observed relative to wildtype DBC2.

Molecular modeling of DBC2's Rho domain indicated that it contains a Lys residue (K27) that is predicted to be in proximity of the γ-phosphate of bound GTP (Fig. 3a). To test this hypothesis the ability of DBC2 and its R99G and V191I mutants to react with desthiobiotin activated GTP, which reacts with and biotinylates Lys within the GTP binding pocket of G-proteins, was examined. [^{35}S]-Labeled DBC2 and its R99G and V191I mutants were synthesized by TnT in RRL, reacted with desthiobiotin activated GTP and pulled-down using NeutrAvidin agarose (Thermo). The amount of radioactivity contained in each reaction was analyzed by scintillation counting of bound [^{35}S]-labeled protein. DBC2, as well R99G and V191I mutants were efficiently labeled with the active desthiobiotin GTP probe (Pierce), demonstrating that the GTP binding pocket of DBC2 and its mutant constructs contained a Lys residue that was indeed positioned near the γ-phosphate of bound GTP as predicted (figure 5b; figure 3a.)

To further examine the specificity of the GTP binding of DBC2 and its R99G and V191I mutants, the ability of excess free GTP to compete for the binding of the proteins to GTP-agarose was examined. [^{35}S]-Labeled DBC2, DBC2/R99G and DBC2/V191I were synthesized by TnT in RRL and pulled-down using GTP-agarose in the presence or absence of excess GTP, and the amounts of radioactivity bound to the GTP-agarose pellets were analyzed through scintillation counting. While a small decrease in the binding of wild-type and R99G DBC2 was observed in the presence of excess GTP, the decrease was not statistically significant (Fig. 5c). However, DBC2/V191I was observed to have a significant reduction (~50%) in its binding to GTP-agarose in the presence of excess GTP (Fig. 5c).

To examine whether the R99G or V191I mutations of DBC2 affected their interaction with components of the Hsp90 machine, [^{35}S]-labeled Flag-tagged DBC2, DBC2/R99G and DBC2/V191I were synthesized by TnT in RRL. Samples were immuno-absorbed with anti-Flag antibody-bound agarose in the presence or absence of geldanamycin, molybdate or vehicle controls, and analyzed for co-adsorbing proteins by SDS-PAGE and Western blotting. The results indicated that the R99G and V191I DBC2 mutants interacted with Hsp90, Hsp70 and HOP, for the most part, in a manner similar to wildtype DBC2 (Fig. 5d). However, in the presence of geldanamycin, DBC2/V191I showed a reduction in bound Hsp90 compared to both that wild-type and R99G DBC2.

Subsequently, the effect of geldanamycin on the ability of the R99G and V191I DBC2 mutants to bind to GTP was examined. [^{35}S]-Labeled DBC2, DBC2/R91G and DBC2/V191I were synthesized and bound to GTP-agarose in the presence of geldanamycin or DMSO as described previously. The binding of DBC2/R99G and

DBC2/V191I to GTP agarose was reduced to the same extent as wild-type DBC2 in the presence of geldanamycin, and the observed reduction in binding was statistically significant (Fig. 5e). Interestingly, while geldanamycin reduced the binding of Hsp90 to DBC2/V191I relative to DBC2 and DBC2/R99G the reduction in GTP binding was similar to the reduction in the GTP binding of wild-type and R99G DBC2 proteins.

A

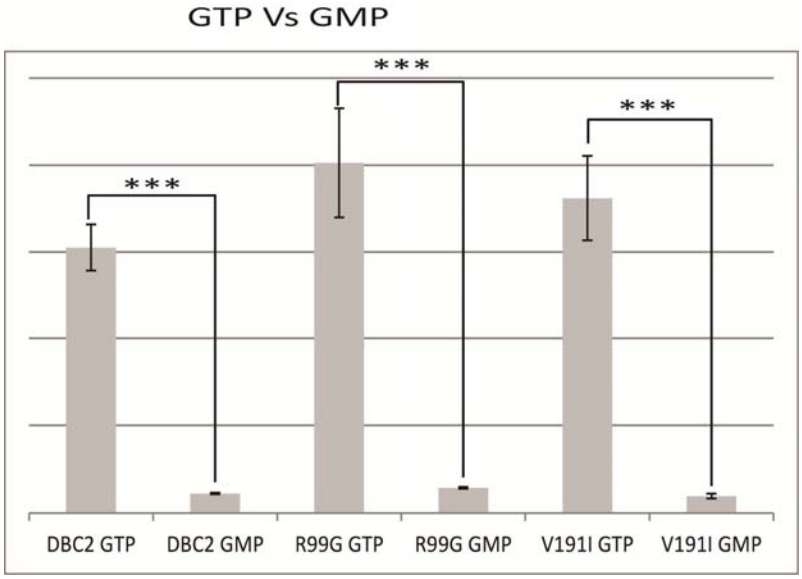
GTP Vs GMP
***
***
***
DBC2 GTP
DBC2 GMP
R99G GTP
R99G GMP
V191I GTP
V191I GMP

B

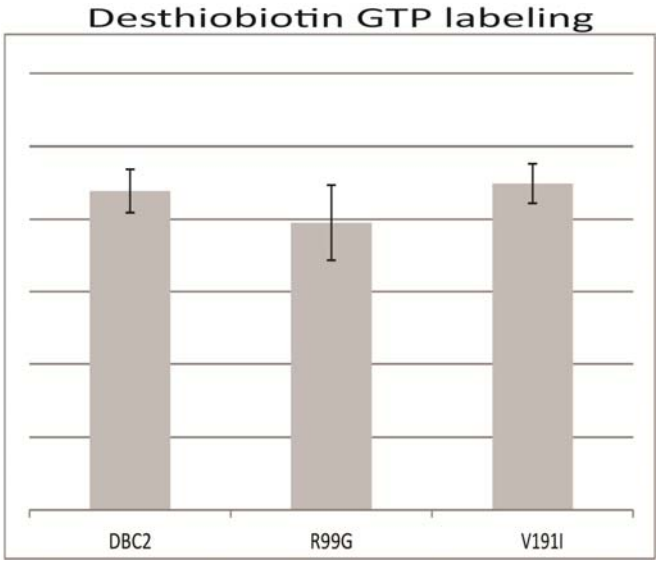
Desthiobiotin GTP labeling
DBC2
R99G
V191I

C

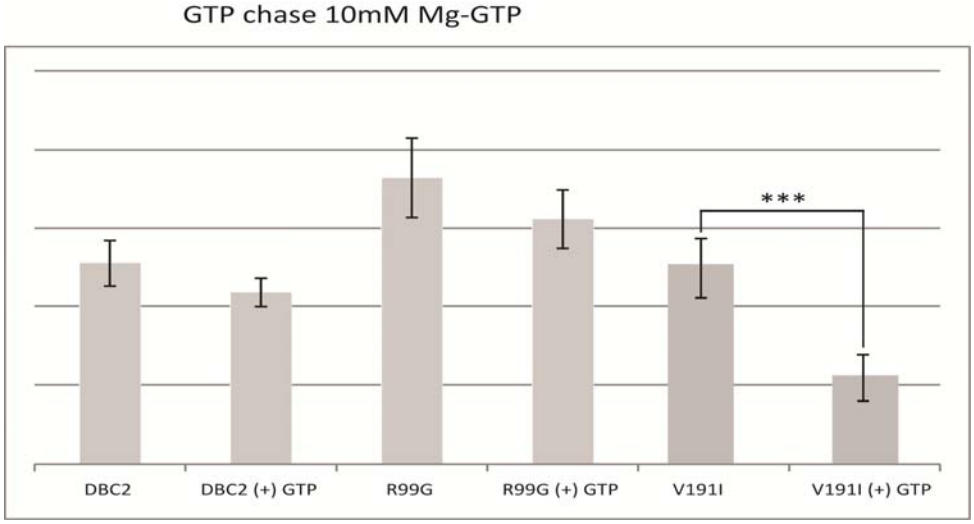
GTP chase 10mM Mg-GTP
***
DBC2
DBC2 (+) GTP
R99G
R99G (+) GTP
V191I
V191I (+) GTP

D

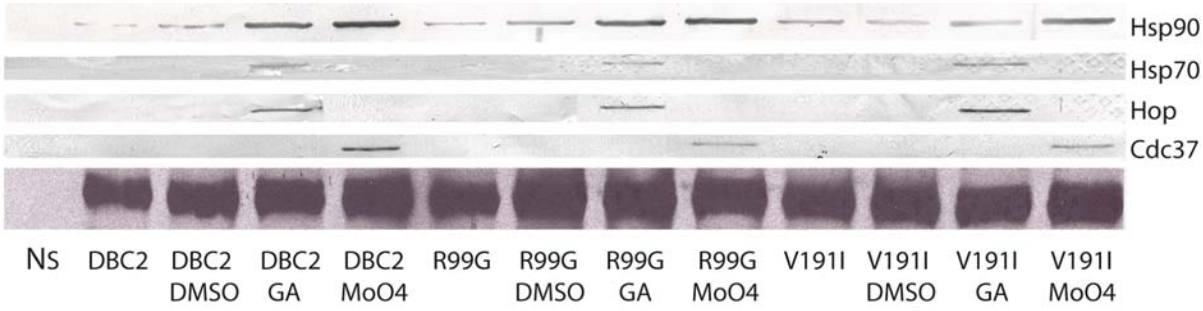

E

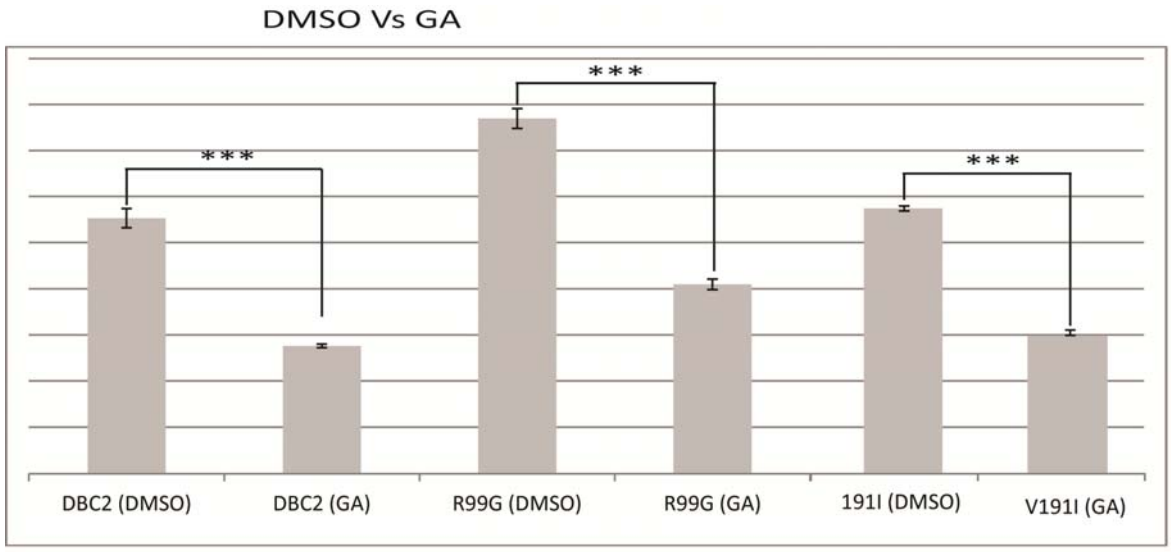

Figure 5: **The effects of mutants inside the Rho domain of DBC2.** [^{35}S]-Labeled WT DBC2, R99G and V191I were generated by T7 PCR TnT followed incubation with GTP-agarose, (A, C, E) GMP-agarose (A) or (B) Neutravidin agarose. The GTP-agarose pellets were then washed as described in Experimental procedures. The amount of bound [^{35}S]-DBC2 proteins were quantitated by scintillation counting and normalized for [^{35}S]-Met non-specifically bound to the GTP-agarose as well as the translation effiecency of each construct. The data represent three independent bio-replicates including three technical replicates/bio-replicates. The (***) denotes a significant difference based on a 95% confidence interval, $P<0.05$. (A) Desthiobiotin labeling of each construct with biotin and quantified as stated above. (A) DBC2 constructs GTP versus GMP binding. (B) labeling with active desthiobiotin probe (C) Addition of 10mM GTP prior to the incubation with GTP-agarose. (D) ^{35}S-labeled Flag-tagged DBC2 proteins (Wt, R99G & I191V) were synthesized in the presence or absence of geldanamycin or molybdate and immunoabsorbed from rabbit reticulocyte lysate with anti-Flag antibodies, as described in Experimental procedures. Immunoabsorbed samples were washed with buffer containing low (100 mM NaCl), as described in Experimental procedures. Samples were analyzed by SDS-PAGE, autoradiography (bottom panel) and Western blotting for co-absorption of endogenous Hsp90, Hsp70, Hop and Cdc37 (top to middle panel). (E) T7 PCR TnT in the presence or absence of the Hsp90 inhibitor GA.

Identification of DBC2-associated proteins by LC-MS/MS.

The results presented above indicate that the capacity of DBC2 to bind GTP is modulated by the Hsp90 chaperone machine, as this capacity was decreased or increased in the presence of the Hsp90 inhibitors geldanamycin or molybdate, respectively. Therefore, the effect of geldanmycin and molybdate on the interaction of DBC2 with proteins was examined by LC-MS/MS analysis of anti-Flag pull downs of Flag-tagged DBC2 synthesized in RRL. The effect of geldanamycin and molybdate on the association of DBC2 with components of the Hsp90 machinery were qualitatively similar to their association with DBC2 accessed by Western blotting (Table 2): geldanamycin increased the association of DBC2 with Hsp90, Hsc70 and HOP, components of Hsp90 intermediate complexes, while the Hsp90-DBC2 complexes stabilized by molybdate lacked HOP and had a decrease in bound Hsc70, consistent with molybdate's role in stabilizing late Hsp90 complexes. The previously reported binding of DBC2 to Cul3 was also observed (Wilkins, Ping, & Carpenter, 2004), and confirmed by Western blotting (Fig. 6). The presence of upward laddering of DBC2 was observed (Fig. 2b) and correlated with the ubiquitination of DBC2 in RRL as detected by UBE associated pull-downs (data not shown). The binding of DBC2 to Cul3 appears to be Hsp90 dependent as it was markedly reduced in the presence of geldanamycin, but was observed in the presence of molybdate. The LC-MS/MS analysis also identified the majority of the components of the COP9 signalosome (Table 2). The COP9 signalosome is known to associate with Cul3 and function as a regulator (Kato & Yoneda-Kato, 2009). The COP9 signalosome components have a similar pattern of interaction, and appear to associate with DBC2 upon its release from Hsp90 at the completion of its ATPase cycle, as there

was a significant decrease in the association of COP9 components with DBC2 in the presence of both geldanamycin and molybdate (Table2). The only COP9 component that seemed to persist throughout the Hsp90 cycle was CSN4, which is known to be a component of the CSN4/5/6/7 subcomplex (Enchev, Schreiber, Beuron, & Morris, 2010).

Associated Proteins	Accession #	WT	DMSO	GA	MoO4
RhoBTB2/DBC2	IPI00171950	95	91	123	84
Hsp70	IPI00003865	174	166	392*	129
Sti1/Hop	IPI00013894	2	0	95*	0♣
Hsp90a	IPI00382470	28	11	153*	162∫
Hsp90b	IPI00414676	0	0	81*	70∫
Cullin-3	IPI00014312	42	37	5♠	29
CSN2	IPI00743825	27	6	4	0♣
CSN3	IPI00025721	15◊	4	0	2
CSN4	IPI00171844	33	30	6♠	5♣
CSN5	IPI00009958	14◊	0	0	1♣
CSN7b	IPI00009301	10◊	0	2	2♣
CSN8	IPI00009480	21	7	0	1♣

Table 2. **LC-MS/MS analysis of DBC2 associated proteins in the presence or absence of Hsp90 inhibitors. Flag-tagged** DBC2 was synthesized by TnT in RRL, followed by treatment with geldanamycin (GA), molybdate (MoO_4) and/or vehicle controls (DMSO or WT/buffer) numbers are the cumulative spectra counts associated with each protein for each treatment. DBC2 samples were then incubated with anti-Flag antibody resin. The immunoresin pellets were then washed and analyzed as described in experimental procedures. The LC-MS/MS data was compiled by Scaffold for protein identification in terms of spectral counts (as in Experimental Procedures) and then exported to Microsoft Excel for statistical analysis. The table represents three independent bio-replicates including three technical replicates of each sample. The significant difference based on a 95% confidence interval, $P<0.05$, associated with the appropriate control. *, ∫, ◊, indicates an increase over GA, MoO_4 or Wt, respectively or ♠, ♣ indicate a decrease over GA or MoO_4, respectively.

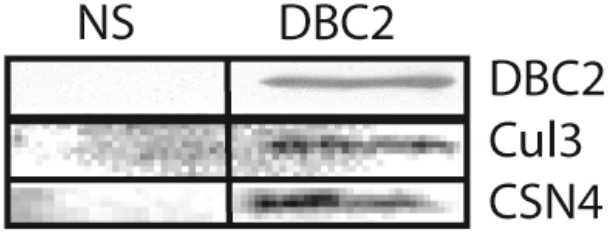

Figure 6. **Western blots of the DBC2-associated components identified by LC-MS/MS**. Flag-tagged DBC2 was synthesized and immunoabsorbed from RRL with anti-Flag antibody agarose, as described in experimental procedures. Immunoabsorbed samples were washed with buffer containing 100 mM NaCl, as described in Experimental procedures. Samples were analyzed by SDS-PAGE, Western blotting for absorption of DBC2 and co-absorption of Cul3 and CSN4.

DBC2 associated proteins isolated from HeLa cell lysates.

While a number of cell lines have been reported to be either sensitive (e.g., MCF7) or resistant (e.g., HeLa) to the growth inhibitory effects of DBC2 expression, little is known about the proteins that associate with DBC2 in these cell lines (Collado, Yoshihara, & Hamaguchi, 2007). DBC2-associated proteins reconstituted from HeLa cell extracts were analyzed by LC-MS/MS, to gain insight into the protein-protein interactions that provide the resistance to the anti-proliferation effect of DBC2 seen in sensitive cells. The majority of the DBC2-associated proteins identified were found to be components of cytoplasmic stress granules (SG) (Anderson et al., 2008, Kimball et al., 2003). The DBC2-associated proteins listed in table 3 represent the major stress granule nucleating proteins and a few major SG DBC2-interacting proteins that were identified. The specific identification of a few of the DBC2-associate SG nucleating proteins (i.e. G3BP1 and TIA-1) along with a major protein involved in processing bodies (PB) (DCP2) are shown in figure 7. The results indicate that DBC2 becomes associated with SGs, as opposed to PBs, as the major associated PB protein is not present in the DBC2 immuno-adsorbed pellet from HeLa cell lysates. In contrast, G3BP1 and TIA-1 were not bound to DBC2 similarly immunoadsorbed from sensitive MCF-7 cell line lysate. Thus, the association of DBC2 with SGs appears a property related to DBC2 resistance, as the SGs nucleating proteins were absent from DBC2 pull downs from sensitive MCF7 extracts (figure 7).

Stress granule	Accession	spectral counts
Ras GTPase-activating protein-binding protein 1 GN=G3BP1	G3BP1_HUMAN	38
Nucleolysin TIA-1 isoform p40 GN=TIA1	TIA1_HUMAN	16
Polyadenylate-binding protein 1 GN=PABPC1	PABP1_HUMAN	87
Fragile X mental retardation syndrome-related protein 1 GN=FXR1	FXR1_HUMAN	16
Zip code-binding protein 1 GN=IGF2BP1	IF2B1_HUMAN	35

Table 3. **LC-MS/MS analysis of DBC2 associated proteins from HeLa cell extracts**. Flag-tagged DBC2 was synthesized by TnT in RRL, followed by mixing with HeLa cell lysate, prepared as described under Experimental procedures. DBC2 samples were then incubated with anti-Flag antibody resins. The immunoresins pellets were then washed and eluted as described in experimental procedures. The LC-MS/MS data was compiled by Scaffold for protein identification and then exported to Microsoft Excel for statistical analysis. The table represents three independent bio-replicates including three technical replicates of each sample. The numbers listed are the cumulative spectra counts associated with each protein. The significant difference based on a 95% confidence interval, $P<0.05$.

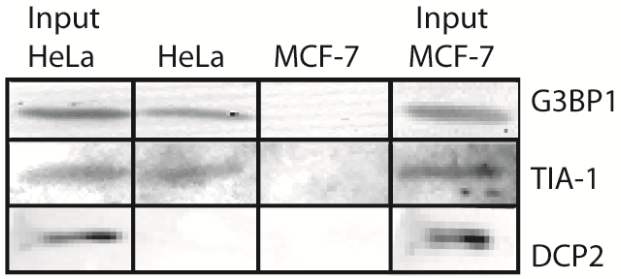

Figure 7. **Western blots of the DBC2-associated components from HeLa cell extracts identified by LC-MS/MS**. Flag-tagged DBC2 was synthesized in RRL, followed by mixing with whole cell HeLa lysate, prepared as described under Experimental procedures. Subsequently, DBC2 was immunoabsorbed with anti-Flag antibody agarose, which was then washed with buffer containing low (150 mM NaCl), and eluted as described under Experimental procedures. Samples were analyzed by SDS-PAGE and Western blotting for G3BP1, TIA-1 and DCP2.

DBC2-associated proteins isolated from MCF-7 cell lysates

To further address the differences in DBC2 protein-protein interactions that may define specific differences between DBC2-resistant and DBC2-sensitive cell lines, DBC2 complexes were reconstituted by incubation of Flag-tagged DBC2 with lysates prepared from sensitive MCF7 cells. The DBC2-associated proteins identified from MCF-7 cells are listed by the category based on functions within the cell (Table 2). As expected, DBC2 was found to be associated with Hsp90α and β isoforms, Hsc70, and two isoforms of DnaJ homologs, as well as p23 (prostaglandin E synthase). In addition, casein kinase 2α/β, a well characterized Hsp90-associate kinase, and endoplasmic reticulum (ER) chaperones, endoplasmin (Grp94), protein disulfide isomerases A4 and A5, and peptidyl-prolyl isomerase B (PPIB) were found to be associated with DBC2.

In the ubiquitin system category, DBC2 associates with Cul3 and an additional E3 ubiquitin ligase (C12orf51). In addition, DBC2 interacts with two components of E3 ligase complexes (damage-specific DNA binding protein 1, DDB1 and calcyclin binding protein, CYBP) and two E2 ligases (UBE2H & O). DBC2 also associated with the COP9 signalosome subunit CSN4, a component of the COP9 signalosome, which is involved in the regulation of Cullin-RING ubiqutin ligases (CRL) complexes (Kato & Yoneda-Kato, 2009).

In the cytoskeleton/ vesicle transport categories DBC2 was found to interact with microtubule motor proteins (Dynein & Myosin) as well as proteins involved in the formation of vesicles (AP-2α, β & AP-3) (McNiven et al., 2006). The DBC2-associated cytoskeletal proteins also included ezrin, a protein whose phosphorylation has been linked to DBC2 anti-proliferation function along with BRMS1 expression (Ling et al.,

2010). Moesin another member of the ERM (erzin, radixin, moesin) protein family (Pfam: ERM (PF00769) was also present. ERMs are cytoskeleton-associated proteins that are known to interact with protein scaffolding associated with the plasma membranes (Fehon et al., 2010).

DBC2 also associates with several proteins that affect cell proliferation along with proteins involved in chromatin remodeling. Among the proteins identified interacting with DBC2 were NPM, TYY1 & TIF1B, three core components of complexes that are involved in chromatin remodeling. Other identified proteins are involved in the process of remodeling in the context of transcription and maintenance of chromosome structure during the cell cycle (e.g., SMC1A/3 components of the cohesion complex.) Overall, DBC2s interaction with these proteins is consistent with its proposed role in modulating gene expression and mitosis (Ling et al., 2010, Freeman et al., 2008, Siripurapu et al., 2005), and supports a role for DBC2 in modulating chromatin remodeling through direct or indirect interactions with the proteins listed above.

Chaperones	Accession	Spectral counts
Casein kinase II subunit alpha OS=Homo sapiens GN=CSNK2A1	CSK21_HUMAN	39
Casein kinase II subunit beta OS=Homo sapiens GN=CSNK2B	CSK2B_HUMAN	19
DnaJ homolog subfamily A member 2 OS=Homo sapiens GN=DNAJA2	DNJA2_HUMAN	10
DnaJ homolog subfamily B member 1 OS=Homo sapiens GN=DNAJB1	DNJB1_HUMAN	29
Endoplasmin OS=Homo sapiens GN=HSP90B1	ENPL_HUMAN	151
Heat shock cognate 71 kDa protein OS=Homo sapiens GN=HSPA8	HSP7C_HUMAN	73
Heat shock protein HSP 90-alpha OS=Homo sapiens GN=HSP90AA1	HS90A_HUMAN	196
Heat shock protein HSP 90-beta OS=Homo sapiens GN=HSP90AB1	HS90B_HUMAN	180
Peptidyl-prolyl cis-trans isomerase B OS=Homo sapiens GN=PPIB	PPIB_HUMAN	164
Prostaglandin E synthase 3 OS=Homo sapiens GN=PTGES3	TEBP_HUMAN	19
Protein disulfide-isomerase A4 OS=Homo sapiens GN=PDIA4	PDIA4_HUMAN	26
Protein disulfide-isomerase A5 OS=Homo sapiens GN=PDIA5	PDIA5_HUMAN	16

Ubiquitin System	Accession	Spectral counts
Calcyclin-binding protein OS=Homo sapiens GN=CACYBP	CYBP_HUMAN	21
COP9 signalosome complex subunit 4 OS=Homo sapiens GN=COPS4	CSN4_HUMAN	5
Cullin-3 OS=Homo sapiens GN=CUL3	CUL3_HUMAN	30
DNA damage-binding protein 1 OS=Homo sapiens GN=DDB1	DDB1_HUMAN	18
Probable E3 ubiquitin-protein ligase C12orf51 OS=Homo sapiens GN=C12orf51	K0614_HUMAN	307
Rho-related BTB domain-containing protein 2 OS=Homo sapiens GN=RHOBTB2	RHBT2_HUMAN	59
Ubiquitin-conjugating enzyme E2 H OS=Homo sapiens GN=UBE2H	UBE2H_HUMAN	40
Ubiquitin-conjugating enzyme E2 O OS=Homo sapiens GN=UBE2O	UBE2O_HUMAN	98

Cytoskelton	Accession	Spectral counts
Adenylyl cyclase-associated protein 1 OS=Homo sapiens GN=CAP1	CAP1_HUMAN	10
Annexin A1 OS=Homo sapiens GN=ANXA1	ANXA1_HUMAN	17
Annexin A2 OS=Homo sapiens GN=ANXA2	ANXA2_HUMAN	115
Cytoskeleton-associated protein 5 OS=Homo sapiens GN=CKAP5	CKAP5_HUMAN	10
Dynein heavy chain 14, axonemal OS=Homo sapiens GN=DNAH14	DYH14_HUMAN	12
Ezrin OS=Homo sapiens GN=EZR	EZRI_HUMAN	170
Glycylpeptide N-tetradecanoyltransferase 1 OS=Homo sapiens GN=NMT1	NMT1_HUMAN	12
Moesin OS=Homo sapiens GN=MSN	MOES_HUMAN	56
Myosin light polypeptide 6 OS=Homo sapiens GN=MYL6	MYL6_HUMAN	13
Myosin-9 OS=Homo sapiens GN=MYH9	MYH9_HUMAN	10
Myosin-VI OS=Homo sapiens GN=MYO6	MYO6_HUMAN	8
N-alpha-acetyltransferase 15, NatA auxiliary subunit OS=Homo sapiens GN=NAA15	NAA15_HUMAN	14
Talin-1 OS=Homo sapiens GN=TLN1	TLN1_HUMAN	12

Vesicle Transport	Accession	Spectral counts
Alpha-taxilin OS=Homo sapiens GN=TXLNA	TXLNA_HUMAN	30
AP-2 complex subunit alpha-1 OS=Homo sapiens GN=AP2A1	AP2A1_HUMAN	8
AP-2 complex subunit beta OS=Homo sapiens GN=AP2B1	AP2B1_HUMAN	14
AP-3 complex subunit beta-1 OS=Homo sapiens GN=AP3B1	AP3B1_HUMAN	13
Protein kinase C and casein kinase substrate in neurons protein 2 OS=Homo sapiens GN=PACSIN2	PACN2_HUMAN	11

Cell Proliferation	Accession	Spectral counts
28 kDa heat- and acid-stable phosphoprotein OS=Homo sapiens GN=PDAP1	HAP28_HUMAN	43
Gamma-taxilin OS=Homo sapiens GN=TXLNG	TXLNG_HUMAN	14
Malignant T cell-amplified sequence 1 OS=Homo sapiens GN=MCTS1	MCTS1_HUMAN	13
Peroxiredoxin-2 OS=Homo sapiens GN=PRDX2	PRDX2_HUMAN	30
Serrate RNA effector molecule homolog OS=Homo sapiens GN=SRRT	SRRT_HUMAN	17

Chromatin Remodeling	Accession	Spectral counts
Basic leucine zipper and W2 domain-containing protein 1 OS=Homo sapiens GN=BZW1	BZW1_HUMAN	17
Basic leucine zipper and W2 domain-containing protein 2 OS=Homo sapiens GN=BZW2	BZW2_HUMAN	26
High mobility group protein B1 OS=Homo sapiens GN=HMGB1	HMGB1_HUMAN	134
High mobility group protein B2 OS=Homo sapiens GN=HMGB2	HMGB2_HUMAN	108
High mobility group protein B3 OS=Homo sapiens GN=HMGB3	HMGB3_HUMAN	22
Histone H1.0 OS=Homo sapiens GN=H1F0	H10_HUMAN	11
Histone H2A type 1-C OS=Homo sapiens GN=HIST1H2AC	H2A1C_HUMAN	26
Histone H2B type 1-M OS=Homo sapiens GN=HIST1H2BM	H2B1M_HUMAN	39
Nucleolin OS=Homo sapiens GN=NCL	NUCL_HUMAN	114
Nucleophosmin OS=Homo sapiens GN=NPM1	NPM_HUMAN	20
Peptidyl-prolyl cis-trans isomerase FKBP3 OS=Homo sapiens GN=FKBP3	FKBP3_HUMAN	69
Poly [ADP-ribose] polymerase 1 OS=Homo sapiens GN=PARP1	PARP1_HUMAN	16
Proliferation-associated protein 2G4 OS=Homo sapiens GN=PA2G4	PA2G4_HUMAN	70
Structural maintenance of chromosomes protein 1A OS=Homo sapiens GN=SMC1A	SMC1A_HUMAN	24
Structural maintenance of chromosomes protein 3 OS=Homo sapiens GN=SMC3	SMC3_HUMAN	32
Transcription intermediary factor 1-beta OS=Homo sapiens GN=TRIM28	TIF1B_HUMAN	17
Transcriptional repressor protein YY1 OS=Homo sapiens GN=YY1	TYY1_HUMAN	14

Table 3. **LC-MS/MS analysis of DBC2-associated proteins isolated from MCF7 cell extracts**. DBC2 was synthesized by TnT in RRL, followed by mixing with whole cell MCF-7 lysate, prepared as described under Experimental Procedures. DBC2 samples were then incubated with anti-Flag antibody resin. The immunoresin pellets were then washed and eluted as described in Experimental procedures. The LC-MS/MS data was compiled by Scaffold for protein identification and then exported to Microsoft Excel for statistical analysis. The table represents three independent bio-replicates including three technical replicates of each sample. The numbers listed are the cumulative spectra counts associated with each protein. The significant difference based on a 95% confidence interval, $P<0.05$, and separated into the categories best suited for the protein group.